DYNAMIC ANALYSIS OF COMPOSITE LAMINATED CIRCULAR PLATE WITH CIRCULAR DELAMINATION

D.-L. Chen*

School of Civil Engineering and Architecture
Changsha University of Science & Technology
Changsha, China

ABSTRACT

In this paper, the effect of delamination on free vibration and primary resonance behaviors of composite circular plate with circular delamination is investigated. Through Reissner Variational Principle, the nonlinear dynamic equilibrium equations, the generalized displacements continuity conditions and the generalized forces equilibrium conditions across delamination front and consistent boundary conditions of delaminated circular plate are obtained. In the work, by introducing Bessel Function and Modified Bessel Function and using Galerkin discretization method, the nonlinear dynamic partial differential equations of delaminated circular plate are transferred into a set of nonlinear ordinary differential equations. Then by using semi-analytic method and multiple scales method, the effects of delamination radius and delamination depth in the thickness-wise on the natural frequency and primary resonance behaviors of delaminated circular plate are presented. The Results show that delamination has considerable effects on the natural frequency and its primary resonance behaviors of delaminated plate.

Keywords: Laminated circular plate, Delamination, Bessel function, Dynamic.

1. INTRODUCTION

In recent years, composite laminated structures have been wildly applied in engineering fields due to their high strength and stiffness-to-weight ratios. However, due to the lack of the thickness reinforcement, various kinds of imperfections, especially delamination, can/will easily occur in composite materials laminated structures. Such imperfections would result in unexpected static and dynamic behavioral changes in engineering structures. According to an experiment study on composite structures subject to dynamic loads [1], the initial delamination and its progressive failure can have negative effects on the dynamic response of structures; therefore, it is important to have a thorough understanding of the dynamic behaviors of the structures with delamination.

For the past three decades analytical and numerical analyses have been carried out by many researchers to analyze delaminated composite structures, including their linear and nonlinear free vibration. The earliest reported study for the vibration analysis of delaminated composite structure was presented by Ramkumar *et al* [2]. They modeled the delaminated beam with a through-width delamination by using four Timoshenko beams. They discussed the effect of delamination on the natural frequencies of a delaminated beam. Later on, Many researchers used 'free mode' [3-4], 'constrained mode' [5-7] and piecewise linear spring model [8-9]assumptions to study the free vibration of delaminated beams. On other side, Chen [10] modeled a composite laminated beam by finite element method to study the effects of delamination length and position on the frequencies. By finite element model, Zak *et al* [11] studied the free vibration of cantilever plates with through width delamination. Shiau *et al* [12] used the finite strip method to investigate the effect of delamination on free vibration of a simply-supported plate with through-width delamination. To avoiding shear and membrane locking phenomenon, Kumar *et al* [13] presented a Mixed Interpolation Tensorial Component, nine node quadrilateral element for studying the free vibration of delamination plate. These mentioned literatures were all focused on one dimensional beam-plate structures with delamination.

However, for two-dimensional plates or shells with embedded delamination, due to the displacement discontinuity at delamination front, it is not convenient to analyze its dynamic behaviors by analytic or semi-analytic method. Thus numerical method is a suitable choice for analyzing the dynamic problem of plates or shells with embedded delamination. Hu *et al* [14] proposed a finite element model to discuss the effect of delamination on the natural frequency and vibration mode shape of a clamped square plate with delamination. Yam *et al* [15]

* Corresponding author (deliang_chen@126.com)

DOI : 10.1017/jmech.2016.84
Copyright © 2016 The Society of Theoretical and Applied Mechanics
https://doi.org/10.1017/jmech.2016.84 Published online by Cambridge University Press

presented a 3-D finite element model to analyze the dynamics of delaminated square plate. Chen *et al* [16] used a mesh-free method to study the free vibration frequencies and mode shapes of delaminated composite beams and plates. By using the orthogonal point collocation method, Chen [17] studied the nonlinear dynamic response of delaminated plates with considering the effect of contact between delamination surface.

In the existing literatures, analytic or semi-analytic method has been rarely applied in the dynamic behavior analysis of delaminated plate with embedded delamination. In the present works, a semi-analytic method is provided, which enables to analysis of the linear and nonlinear dynamic behaviors of delaminated circular plate (embedded delamination) basing on the Galerkin discretization procedure. The research are mainly focused on effect of delamination parameters on the natural frequency, mode shape and primary resonance of delaminated plate.

2. EQUATION FORMULATION

Consider a composite laminated circular plate with radius R, thickness h, and mass density per unit volume γ, the plate has a central circular delamination with radius a and is subject to transverse load $q(r, t)$ with the frequency of Ω as shown in Fig. 1. Due to the discontinuity of displacement at the delamination front, the delaminated circular plate is taken as three regions as shown in the figure, where *II, III* are delaminated regions, and *I* is non-delaminated regions. h, h_{II} and h_{III} are the thicknesses of region *I*, *II*, and *III*, respectively. The origin of the coordinate is located at the circle center of the mid-surface for each region.

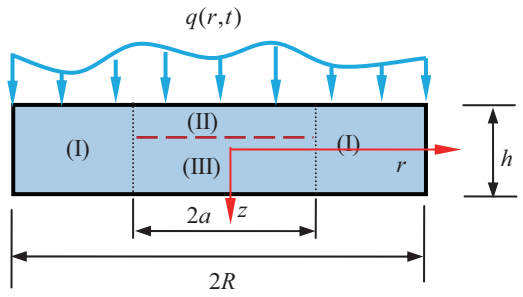


Fig. 1 Configuration of composite laminate circular plate with circular delamination.

According to the first-order shear deformation theory, the displacements of each region can be written as

$$\begin{aligned}\tilde{u}^i(r,z) &= u^i(r) + z\phi^i(r)\\ \tilde{w}^i(r,z) &= w^i(r)\end{aligned} \quad (i = I, II, III) \tag{1}$$

in which, $u^i(r)$, $w^i(r)$ are the displacements at the mid-plane of i region, and $\phi^i(r)$ is the rotation of the normal of mid-plane along the r-axis of i region, $\tilde{u}^i(r,z)$, $\tilde{w}^i(r,z)$ are the displacements of i region at a point (r, z) from the median surface.

Based on the Von Kármán nonlinear strain–displacement relation and the above-mentioned displacement field, the strain components of each region are

$$\begin{Bmatrix}\bar{\varepsilon}_r^i\\ \bar{\varepsilon}_\theta^i\end{Bmatrix} = \begin{Bmatrix}\varepsilon_r^{0i}\\ \varepsilon_\theta^{0i}\end{Bmatrix} + z\begin{Bmatrix}\kappa_r^i\\ \kappa_\theta^i\end{Bmatrix}$$
$$\varepsilon_{rz}^i = \phi^i + w_{,r}^i \tag{2}$$

where

$$\begin{Bmatrix}\varepsilon_r^{0i}\\ \varepsilon_\theta^{0i}\end{Bmatrix} = \begin{Bmatrix}\dfrac{\partial u^i}{\partial r} + \dfrac{1}{2}\left(\dfrac{\partial w^i}{\partial r}\right)^2\\ \dfrac{u^i}{r}\end{Bmatrix}, \qquad \begin{Bmatrix}\kappa_r^i\\ \kappa_\theta^i\end{Bmatrix} = \begin{Bmatrix}\dfrac{\partial \phi^i}{\partial r}\\ \dfrac{\phi^i}{r}\end{Bmatrix}$$

For a cylindrical orthotropic circular plate laminated symmetrically with respect to the middle surface, the generalized stress-strain relations of i-region are expressed as follows

$$\begin{Bmatrix}\boldsymbol{N}^i\\ \boldsymbol{M}^i\end{Bmatrix} = \begin{bmatrix}\boldsymbol{A}^i & 0\\ 0 & \boldsymbol{D}^i\end{bmatrix}\begin{Bmatrix}\boldsymbol{\varepsilon}^{0i}\\ \boldsymbol{\kappa}^i\end{Bmatrix}$$
$$Q_r^i = C_{44}{}^i\varepsilon_{rz}^i \tag{3}$$

where A^i, D^i are the extensional and flexural stiffness matrix of i-region of delaminated plate.

By using inverse transform of Eq.(3), we have

$$\begin{Bmatrix}\boldsymbol{\varepsilon}^{0i}\\ \boldsymbol{M}^i\end{Bmatrix} = \begin{bmatrix}\boldsymbol{A}^{*i} & 0\\ 0 & \boldsymbol{D}^{*i}\end{bmatrix}\begin{Bmatrix}\boldsymbol{N}^i\\ \boldsymbol{\kappa}^i\end{Bmatrix}$$
$$\varepsilon_{rz}^i = C_{44}^{*}{}^i Q_r^i \tag{4}$$

in which

$$\boldsymbol{A}^{*i} = (\boldsymbol{A}^i)^{-1}, \quad \boldsymbol{D}^* = \boldsymbol{D}, \quad C_{44}^{*i} = (C_{44}^i)^{-1} = \frac{2}{1-\upsilon}A_{11}^{*i}.$$

The 'free mode' is used to model the delamination problem of the circular plate, so the total potential energy of the delaminated circular plates under uniform loads can be expresses as follows

$$\begin{aligned}\Pi &= \sum_{i=I}^{III}\iiint_{V_i} A(e_{\alpha\beta})dV_i - \sum_{i=I}^{III}\iint_{A_i} q^i(r,t)w^i dA - \sum_{j=1}^{3}\sum_{i=I}^{III}\iiint_{V_i} A(e_{\alpha\beta})f_j^i u_j^i dV_i\\ &= \sum_{i=I}^{III}\iint_{A_i}\left(\begin{Bmatrix}[N^i]\\ [M^i]\end{Bmatrix}^T\begin{Bmatrix}\varepsilon^{0i}\\ \kappa^i\end{Bmatrix} + Q_r^i\varepsilon_{rz}^i\right)rdrd\theta - \sum_{i=I}^{III}\iint_{A_i} q^i(r,t)w^i dA - \sum_{j=1}^{3}\sum_{i=I}^{III}\iiint_{V_i} A(e_{\alpha\beta})f_j^i u_j^i dV_i\end{aligned} \tag{5}$$

https://doi.org/10.1017/jmech.2016.84 Published online by Cambridge University Press

where, $A(e_{\alpha\beta})$ is the potential energy density in unit volume V_i, f_1^i, f_2^i, f_3^i represents the inertial force $\rho_0 u_{,tt}^i$, $\rho_0 w_{,tt}^i$, $\rho_0 \phi_{,tt}^i$ of region-*i*, respectively. u_1^i, u_2^i, u_3^i represents the displacements u^i, w^i, ϕ^i of region-*i*, respectively. γ is the mass density per unit volume of plate.

By applying Reissiner Variational Principle, via Eq. (5), the nonlinear governing equations of *i* region of the delaminated circular plate are derived as

$$\begin{aligned}
&N_{r,r}^i + \frac{N_r^i - N_\theta^i}{r} = \gamma h_i u_{,tt}^i \\
&\frac{1}{r}\left[\frac{\partial}{\partial r}(rM_r^i) - M_\theta^i - rQ_r^i\right] = \frac{\gamma h_i^3}{12}\phi_{,tt}^i \\
&\frac{1}{r}\frac{\partial}{\partial r}[r(Q_r^i + N_r^i w_{,r}^i) = -q^i(r,t) + \gamma h_i w_{,tt}^i + c w_{,t}^i
\end{aligned} \tag{6}$$

For a circular plate structure, the in-plane inertia term $u_{,tt}^i$ is very small compared with transverse inertia term $w_{,tt}^i$, then the term $u_{,tt}^i$ might be neglected. Then Eq. (6) can be rewritten as.

$$\begin{aligned}
&N_\theta^i = rN_{r,r}^i + N_r^i \\
&Q_r^i = \frac{1}{r}\left[\frac{\partial}{\partial r}(rM_r^i) - M_\theta^i\right] - \frac{\gamma h_i^3}{12}\phi_{,tt}^i \\
&\frac{1}{r}\frac{\partial}{\partial r}\left[\frac{\partial}{\partial r}(rM_r^i) - M_\theta^i + rN_r^i w_{,r}^i - \frac{\gamma h_i^3}{12}\phi_{,tt}^i\right] = -q^i(r,t) + \gamma h_i w_{,tt}^i + c w_{,t}^i
\end{aligned} \tag{7}$$

By using the relationship $\varepsilon_r^{0i} = \frac{\partial u^i}{\partial r} + \frac{1}{2}(w_{,r}^i)^2$ and $u^i = r\varepsilon_\theta^{0i}$, the strain compatibility equation in middle plane of circular plane can be derived as

$$\varepsilon_r^{0i} = \varepsilon_\theta^{0i} + r\varepsilon_{\theta,r}^{0i} + \frac{1}{2}(w_{,r}^i)^2 \tag{8}$$

Combining Eq. (3-4), Eq. (7) and Eq. (8). After some algebraic transformation the governing equations Eq. (7) of delaminated circular plates can be rewritten as

$$\begin{aligned}
&\frac{1}{r}\frac{\partial}{\partial r}(rN_r^i w_{,r}^i) + D_{11}^{*\,i}\phi_{,rrr}^i + \frac{2}{r}D_{11}^{*\,i}\phi_{,rr}^i - \frac{1}{r^2}D_{22}^{*\,i}\phi_{,r}^i + \frac{1}{r^3}D_{22}^{*\,i}\phi^i = \gamma h_i w_{,tt}^i + \frac{\gamma h_i^3}{12}\phi_{,tt}^i + \frac{\gamma h_i^3}{12}\phi_{,rtt}^i - q^i(r,t) + c w_{,t}^i \\
&\phi^i + w_{,r}^i = C_{44}^{*\,i}\left[D_{11}^{*\,i}\phi_{,rr}^i + \frac{1}{r}D_{11}^{*\,i}\phi_{,r}^i - \frac{2}{r^2}D_{22}^{*\,i}\phi^i - \frac{\gamma h_i^3}{12r}\phi_{,tt}^i\right] \\
&A_{22}^{*\,i} r^2 N_{r,rr}^i + 3A_{22}^{*\,i} r N_{r,r}^i + (A_{22}^{*\,i} - A_{11}^{*\,i})N_r^i + \frac{1}{2}w_{,r}^{i\,2} = 0
\end{aligned} \tag{9}$$

The boundary conditions and natural conditions of circular plate centrality can be expressed as

$$r = R,\ \ w^I(t) = 0, N^I(t) = 0, M^I(t) = K\phi^I(t) \tag{10}$$

$$r = 0,\ \ Q^i(t) = 0,\quad N^i(t) \text{ finite value},\quad \phi^i(t) = 0 \quad (i = II, III) \tag{11}$$

in which, K is the Elastic support coefficient of the outer boundary. $K = 0$ denotes a simply-supported boundary conditions，and $K = \infty$ denotes fixed boundary conditions.

The generalized displacement continuity conditions across the delamination front can be written as

$$\begin{aligned}
&w^I(a,t) = w^{II}(a,t),\ w^I(a,t) = w^{III}(a,t) \\
&\phi^I(a,t) = \phi^{II}(a,t), \phi^I(a,t) = \phi^{III}(a,t) \\
&u^{II}(a,t) - u^I(a,t) + \phi^I(a,t)h_{III}/2 = 0, u^{III}(a,t) - u^I(a,t) - \phi^I(a,t)h_{II}/2 = 0
\end{aligned} \tag{12}$$

The equilibrium conditions of the generalized force continuity conditions at the delamination front can be denoted as

https://doi.org/10.1017/jmech.2016.84 Published online by Cambridge University Press

$$
\begin{aligned}
&N_r^I(a,t)=N_r^{II}(a,t)+N_r^{III}(a,t)\\
&Q_r^I(a,t)=Q_r^{II}(a,t)+Q_r^{III}(a,t)\\
&M_r^I(a,t)-M_r^{II}(a,t)-M_r^{III}(a,t)-[N_r^{II}(a,t)h_{III}-N_r^{III}(a,t)h_{II}]/2=0
\end{aligned}
\tag{13}
$$

In order to re-express the governing equations, boundary conditions and continuity conditions at the delamination front in dimensionless form, the following parameters are introduced

$$
\begin{aligned}
&\rho=\frac{r}{R},\quad \bar{w}^i=\frac{w^i}{h},\quad \bar{\phi}^i=\frac{R}{h}\phi^i,\quad \bar{N}_\rho^i=\frac{R}{D_{11}^I}rN_r^i,\quad \xi=\frac{h_I}{R},\quad \rho_0=\frac{a}{R},\quad \bar{K}=\frac{RK}{D_{11}^I}\\
&\alpha_1^i=\frac{D_{11}^i}{D_{11}^I},\quad \alpha_2^i=\frac{A_{22}^{*i}}{A_{22}^{*I}},\quad \alpha_3^i=\frac{A_{21}^{*i}}{A_{22}^{*I}},\quad \alpha_4^i=\frac{A_{11}^{*i}}{A_{22}^{*I}},\quad \alpha_5^i=\frac{D_{12}^i}{D_{11}^I},\quad \alpha_6^i=\frac{D_{22}^i}{D_{11}^I}\\
&\beta_1^i=\frac{R^2}{C_{44}^{*i}D_{11}^I},\quad \beta_2^i=\frac{h^2}{D_{11}^I A_{22}^{*i}},\quad \lambda_2=\frac{h_{II}}{h},\quad \lambda_3=\frac{h_{III}}{h},\quad \bar{N}_0=\frac{R^2}{D_{11}^I}N_0\\
&\bar{q}^i(\rho,\tau)=\frac{R^4}{D_{11}^I h_I}F^i(x,t),\quad \bar{c}^i=c^i\sqrt{\frac{R^2h}{D_{11}^I\rho_0}},\quad \tau=\frac{t}{R^2}\sqrt{\frac{D_{11}^I}{\gamma h_I}},\quad \eta_1=\frac{D_{11}^I}{R^4k},\quad \eta_2=\frac{D_{11}^I}{R^4k_h h_I^{1/2}}
\end{aligned}
\tag{14}
$$

By substituting Eq. (1) into Eqs. (9)-(13), one can get the dimensionless nonlinear differential equations of the delaminated plate as follows

$$
\begin{aligned}
&\alpha_1^i\bar{\phi}^i_{,\rho\rho\rho}+2\alpha_1^i\frac{1}{\rho}\bar{\phi}^i_{,\rho\rho}-\alpha_6^i\frac{1}{\rho^2}\bar{\phi}^i_{,\rho}+\alpha_6^i\frac{1}{\rho^3}\bar{\phi}^i+\frac{1}{\rho}\frac{\partial}{\partial\rho}(\bar{N}_\rho^i\bar{w}^i_{,\rho})=\lambda_i\bar{w}^i_{,\tau\tau}+\frac{1}{12\rho}\xi^2\lambda_i\bar{\phi}^i_{,\tau\tau}+\frac{1}{12}\xi^2\lambda_i\bar{\phi}^i_{,\tau\tau}-T_L^i\bar{q}^i(r,\tau)+\bar{c}^i\bar{w}^i_{,\tau}\\
&\alpha_1^i\bar{\phi}^i_{,\rho\rho}+\alpha_1^i\frac{1}{\rho}\bar{\phi}^i_{,\rho}-\alpha_6^i\frac{1}{\rho^2}\bar{\phi}^i-\frac{1}{12\rho}\xi^2\lambda_i\bar{\phi}^i_{,\tau\tau}=\beta_1^i(\bar{\phi}^i+\bar{w}^i_{,\rho})\quad (i=I,II,III)\\
&\alpha_2^i\rho\bar{N}^i_{\rho,\rho\rho}+3\alpha_2^i\bar{N}^i_{\rho,\rho}+(\alpha_2^i-\alpha_4^i)\frac{1}{\rho}\bar{N}_\rho^i+\frac{1}{2}\beta_2^i\bar{w}^i_{,\rho}{}^2=0
\end{aligned}
\tag{15}
$$

in which, $T_L^i=0\ (i=III)$ and $T_L^i=1\ (i=I,II)$

Dimensionless boundary conditions and natural conditions of circular plate centrality are given as

$$
\bar{w}^I(1,\tau)=0,\quad \bar{N}^I(1,\tau)=0,\quad \bar{\phi}^I(1,\tau)+\frac{1}{\rho}\alpha_5^I\bar{\phi}^I(1,\tau)=\bar{K}\bar{\phi}(1,\tau)
\tag{16}
$$

$$
\bar{\phi}^i(0,\tau)+\bar{w}^i_{,\rho}(0,\tau)=0,\quad \bar{\phi}^i(0,\tau)=0,\quad \bar{N}_\rho^i(0,\tau)\ \text{ finite value } (i=II,III)
\tag{17}
$$

Dimensionless displacements continuity conditions across the delamination front ($\rho=\rho_0$) are derived as

$$
\begin{aligned}
&\bar{w}^I(\rho_0,\tau)=\bar{w}^{II}(\rho_0,\tau)\quad \bar{w}^I(\rho_0,\tau)=\bar{w}^{III}(\rho_0,\tau)\\
&\bar{\phi}^I(\rho_0,\tau)=\bar{\phi}^{II}(\rho_0,\tau)\quad \bar{\phi}^I(\rho_0,\tau)=\bar{\phi}^{III}(\rho_0,\tau)
\end{aligned}
\tag{18}
$$

Dimensionless equilibrium conditions of the generalized force continuity conditions at the delamination front are given in the following

$$
\begin{aligned}
&(\alpha_3^{II}+\alpha_2^{II})\bar{N}_\rho^{II}(\rho_0,\tau)+\alpha_2^{II}\rho_0\bar{N}^{II}_{\rho,\rho}(\rho_0,\tau)-[(\alpha_3^I+\alpha_2^I)\bar{N}_\rho^I(\rho_0,\tau)+\alpha_2^I\rho_0\bar{N}^I_{\rho,\rho}(\rho_0,\tau)]-\frac{1}{2}\lambda_3\beta_2^I\bar{\phi}^I(\rho_0,\tau)=0\\
&(\alpha_3^{III}+\alpha_2^{III})\bar{N}_\rho^{III}(\rho_0,\tau)+\alpha_2^{II}\rho_0\bar{N}^{III}_{\rho,\rho}(\rho_0,\tau)-[(\alpha_3^I+\alpha_2^I)\bar{N}_\rho^I(\rho_0,\tau)+\alpha_2^I\rho_0\bar{N}^I_{\rho,\rho}(\rho_0,\tau)]+\frac{1}{2}\lambda_2\beta_2^I\bar{\phi}^I(\rho_0,\tau)=0
\end{aligned}
\tag{19}
$$

$$
\begin{aligned}
&\bar{N}_\rho^I(\rho_0,\tau)=\bar{N}_\rho^{II}(\rho_0,\tau)+\bar{N}_\rho^{III}(\rho_0,\tau)\\
&\beta_1^I[\phi^I(\rho_0,\tau)+\bar{w}^I_{,\rho}(\rho_0,\tau)]=\beta_1^{II}[\phi^{II}(\rho_0,\tau)+\bar{w}^{II}_{,\rho}(\rho_0,\tau)]+\beta_1^{III}[\phi^{III}(\rho_0,\tau)+\bar{w}^{III}_{,\rho}(\rho_0,\tau)]\\
&\bar{\phi}^I_{,\rho}(\rho_0,\tau)+\frac{1}{\rho_0}\alpha_5^I\bar{\phi}^I(\rho_0,\tau)-\left[\alpha_1^{II}\bar{\phi}^{II}(\rho_0,\tau)+\frac{1}{\rho_0}\alpha_5^{II}\bar{\phi}^{II}(\rho_0,\tau)\right]-\left[\alpha_1^{III}\bar{\phi}^{III}_{,\rho}(\rho_0,\tau)+\frac{1}{\rho_0}\alpha_5^{III}\bar{\phi}^{III}(\rho_0,\tau)\right]\\
&-\left[\frac{1}{\rho_0}\lambda_3\bar{N}_\rho^{II}(\rho_0,\tau)-\frac{1}{\rho_0}\lambda_2\bar{N}_\rho^{III}(\rho_0,\tau)\right]/2=0
\end{aligned}
$$

To study the nonlinear dynamic response of composite laminated circular plate with delamination, the following rela-

https://doi.org/10.1017/jmech.2016.84 Published online by Cambridge University Press

tionships are introduced

$$w^i(\rho,\tau)=\sum_{n=1}^{\infty}W_n(\tau)G_n^i(\rho)$$
$$\phi^i(\rho,\tau)=\sum_{n=1}^{\infty}\Phi_n(\tau)G_n^i{}'(\rho) \tag{20}$$
$$N^i(\rho,\tau)=\sum_{n=1}^{\infty}N_n(\tau)F_n^i(\rho)$$

where $G_n^i(\rho)$, $F_n^i(\rho)$ are the vibration modes of *i*-region, and we have

$$G_n^i(\rho)=A_n^iJ_n(\alpha_n\rho)+B_n^iY_n(\alpha_n\rho)+\rho[C_n^iI_n(\alpha_n\rho)+D_n^iK_n(\alpha_n\rho)]$$
$$F_n^i(\rho)=E_n^i\rho J_n(\beta_n\rho)+F_n^i \tag{21}$$

in which $J_n(\alpha_n\rho)$ and $Y_n(\alpha_n\rho)$ are Bessel Function of the first and second kind, respectively. $I_n(\alpha_n\rho)$ and $K_n(\alpha_n\rho)$ are modified Bessel Function of the first and second kind, respectively. Coefficients $A_n^i, B_n^i, C_n^i, D_n^i, E_n^i, F_n^i, \alpha_n, \beta_n$ can be determined by the boundary conditions, displacements and generalized force continuity conditions at the delamination front (see Appendix A). After that, the vibration mode function of the delaminated circular plate can be obtained.

Applying Galerkin procedure to the differential governing equations Eq. (15), it yields

$$\sum_{n=1}^{\infty}a_{nk}^1\ddot{W}_n(\tau)+\sum_{n=1}^{\infty}a_{nk}^2\ddot{\Phi}_n(\tau)+\sum_{n=1}^{\infty}a_{nk}^3\dot{W}_n(\tau)+\sum_{n=1,m=1}^{\infty}a_{nmk}^4N_n(\tau)W_m(\tau)+\sum_{n=1}^{\infty}a_{nk}^5\Phi_n(\tau)=F_k(\tau)$$
$$\sum_{n=1}^{\infty}a_{nk}^6\ddot{\Phi}_n(\tau)+\sum_{n=1}^{\infty}a_{nk}^7\Phi_n(\tau)+\sum_{n=1}^{\infty}a_{nk}^8W_n(\tau)=0 \tag{22}$$
$$\sum_{n=1}^{\infty}a_{nk}^9N_n(\tau)+\sum_{n=1,m=1}^{\infty}a_{nmk}^{10}W_n(\tau)W_m(\tau)=0$$

where the coefficient are given in Appendix B.

Only considering the first-order vibration of delaminated circular plate, and omitting the inertia term $\ddot{\Phi}(\tau)$, then the terms $\Phi(\tau), N(\tau)$ can be eliminated. For brevity, the subscripts of the coefficients a_{nk}^i, a_{nmk}^i and time terms in Eq. (21) are omitted. Then Eq. (22) can be rewritten as

$$\ddot{W}(\tau)+\Gamma_1W(\tau)+\Gamma_2\dot{W}(\tau)+\Gamma_3W^3(\tau)=\tilde{F}(\tau) \tag{23}$$

where

$$\Gamma_1=-\frac{a^5a^8}{a^1a^7},\quad \Gamma_2=-\frac{a^3}{a^1},\quad \Gamma_3=-\frac{a^4a^{10}}{a^1a^9},\quad \tilde{F}(\tau)=\frac{1}{a^1}F(\tau) \tag{24}$$

3 NUMERICAL SIMULATIONS AND DISCUSSIONS

In the following, a clamped supported symmetric cylindrical orthotropic laminated delamination circular plate with Glass-epoxy is considered, which consists of 21 layers with the identical thickness (0.0025 m). The material properties of circular plate are E_r = 17.93 GPa, E_θ = 53.8 GPa, $G_{r\theta}$= 8.96 GPa, ν = 0.25. The radius is R = 1.0 m and the height is h = 0.0525 m.

3.1 The Effect of Delamination on Natural Frequency of Laminated Circular Plate

Before starting the analysis in this section, the effectiveness of the proposed semi-analytical method needs to be verified. From Eq. (23), the dimensionless natural frequency of homogeneous circular plate is derived as 10.193, which well matches the result 10.216 [Ref. 18].

The dimensionless frequencies of circular plates with various delamination radii and depths are investigated as shown in Table 1.

Table 1 presents the influence of delamination radius ρ_0 and delamination depth λ_2 on the natural frequency of a Glass-epoxy circular plate with a central circular delamination. It shows that the natural frequency of delaminated plate decreases rapidly with the increase in the delamination radius ρ_0, and the it will decrease drastically especially at the small delamination depth λ_2 (The

https://doi.org/10.1017/jmech.2016.84 Published online by Cambridge University Press

Table 1 The frequencies of laminated circular plate with different delamination radii and depths

Delamination radius ρ_0		0.1	0.2	0.3	0.4	0.5	0.6	0.7	0.8	0.9
Delamination depth λ_2	2/21	10.995	10.857	10.339	6.7390	4.376	3.085	2.157	1.689	1.393
	5/21	10.998	10.877	10.346	9.860	8.620	6.756	5.107	3.922	3.172
	10/21	11.005	10.895	10.369	10.044	9.741	9.123	8.204	7.038	5.915

delamination is close to the surface of plate). Moreover, the natural frequency of a delamination plate will also decrease with the decrease in the delamination depth λ_2.

Combining the mode function $G_n^i(\rho)$ of i-region, boundary conditions and displacement and generalized force conditions at delamination front, one can get the mode shape of a delaminated circular plate as shown in Figs. 2-4.

Figure 2 shows the mode shape with various delamination radii at small delamination depth $\lambda_2 = 2/21$ (shallow delamination). Here only the r-direction shape of mode shape of the delaminated circular plate is shown. For the small delamination radius $\rho_0 = 0.2$, the global mode dominates (Region II and Region III have the same order of magnitude) the mode shape of the delaminated circular plate. For the medium delamination radius $\rho_0 = 0.5$ and large delamination radius $\rho_0 = 0.8$, the local mode (The order of magnitude of Region II is much larger than that of Region III, and the magnitudes of Region I and III are of the same order) will dominate the mode shape of the delaminated circular plate.

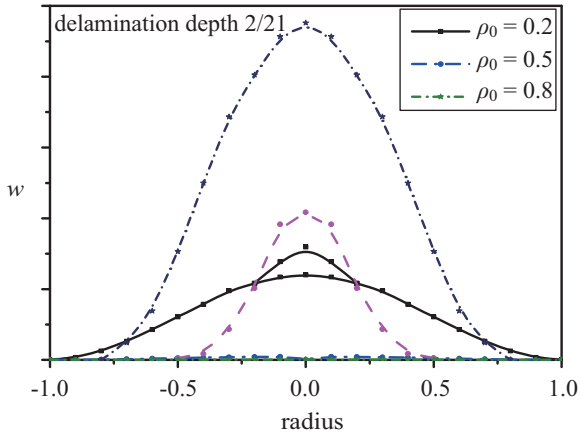


Fig. 2 Mode shape of delaminated plate with various delamination radii ($\lambda_2 = 2/21$).

At the medium delamination depth $\lambda_2 = 5/21$, the mode shape of a delaminated circular plate with various delamination radii is displayed in Fig. 3. As shown in Fig. 3, when the delamination occurs at the medium depth $\lambda_2 = 5/21$, the mode shape of the delaminated circular plate will dominate global mode in the case of the small delamination radius $\rho_0 = 0.2$. For medium delamination radius $\rho_0 = 0.5$, the mode shape of the delaminated circular plate will be featured as global mode plus the local mode (The magnitude of Region II is still much larger than that of Region III, while their magnitudes are of the same order). For the large delamination radius $\rho_0 = 0.8$, the local mode dominates the mode shape of the delaminated circular plate.

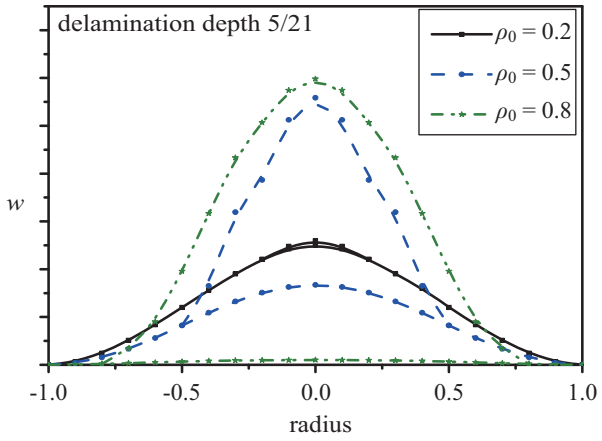


Fig. 3 Mode shape of delaminated plate with various delamination radii ($\lambda_2 = 5/21$).

When the delamination occurs at the large depth $\lambda_2 = 10/21$ (deep delamination), the mode shape of delaminated circular plate with different delamination radii is presented in Fig. 4. It can be seen, at this case, the global mode dominates the mode shape of delaminated circular plate for small and medium delamination radius, For the large delamination radius $\rho_0 = 0.8$, the mode shape of the delaminated plate will be global mode superposing the local mode.

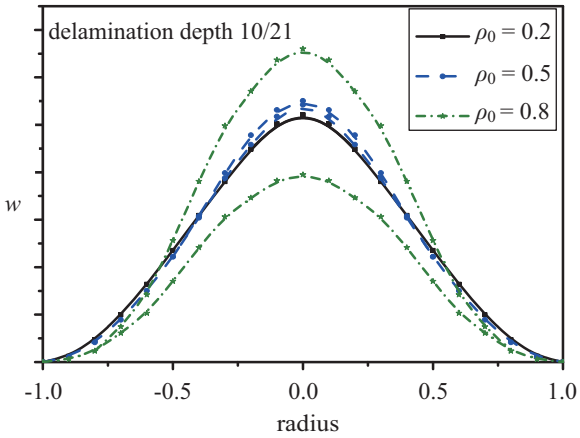


Fig. 4 Mode shape of delaminated plate with various delamination radii ($\lambda_2 = 10/21$).

From Figs. 2-4, one can conclude that both the delamination depth and radius affect the mode shape of the delaminated circular plate. However, in the case of

https://doi.org/10.1017/jmech.2016.84 Published online by Cambridge University Press

small delamination radius, the global mode dominates the mode shape of the delaminated circular plate whatever the delamination depth it is. On the other hand, the local mode will dominate the mode shape of the delaminated circular plate at the large delamination radius and small delamination depth. Besides, the effect of delamination radius and depth on the natural frequency of delaminated circular plate can also be explained from the plots of mode shape shown in Figs. 2-4.

3.2 The Effect of Delamination on Primary Resonance Behaviors of Circular Plate

In the following, the primary resonance of delaminated circular plate is investigated. In order to characterize the contribution of the nonlinear terms and damping effect, a small dimensionless perturbation parameter ε is introduced. The external excitation in Eq. (23) is hypothesized as $\tilde{F}(\tau) = F_0(\tau)\cos\Omega t$. Then Eq. (23) can be re-written as the following forced Duffing System,

$$\ddot{W}_1(\tau) + \omega_0^2 W_1(\tau) + 2\varepsilon\mu\dot{W}_1(\tau) + \varepsilon\gamma W_1^3(\tau) = \varepsilon f\cos\Omega t \quad (25)$$

in which,

$$\omega_0^2 = \Gamma_1,\ \varepsilon\gamma = \Gamma_3,\ \varepsilon\mu = \Gamma_2,\ \varepsilon f\cos\Omega t = F_0(\tau)\cos\Omega t\ .$$

The method of multiple scales in Ref. [19] is used to solve Eq. (25). Through a series of transformations, the frequency response equation of the delaminated circular plate can be obtained as

$$\frac{f^2}{4\omega_0^2} = \mu^2 a^2 + \left(a\sigma - \frac{3\gamma a^3}{8\omega_0}\right)^2 \quad (26)$$

in which, σ, the detuning parameter is introduced to describe the relationship between Ω and ω_0 in the form of $\Omega = \omega_0 + \varepsilon\sigma$. From Eq. (23), the frequency-response graphs are drawn in Figs. 5-6 in the case of $f = 200$ and $\mu = 0.2$. The frequency-response graphs corresponding to various delamination radii are given in Fig. 5 for the delamination depth $\lambda_2 = 10/21$. Figure 5 shows that the increase in the delamination radius will enlarge the hardening type behaviors.

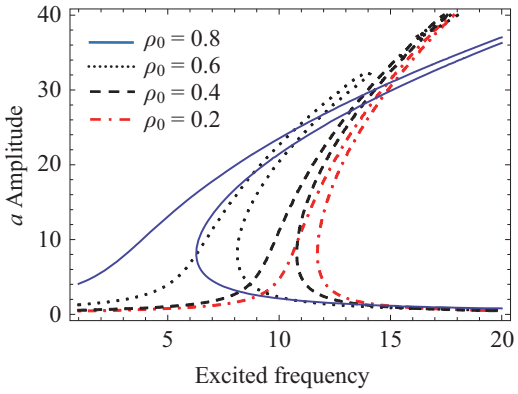


Fig. 5 Force-response curves of delaminated plate corresponding to different delamination radii.

Figure 6 shows the frequency-response graphs of delaminated circular plate with different delamination depths, in the case of the delamination radius $\rho_0 = 0.5$. One can conclude that the increase in the delamination depth λ_2 will also enlarge the hardening type behaviors.

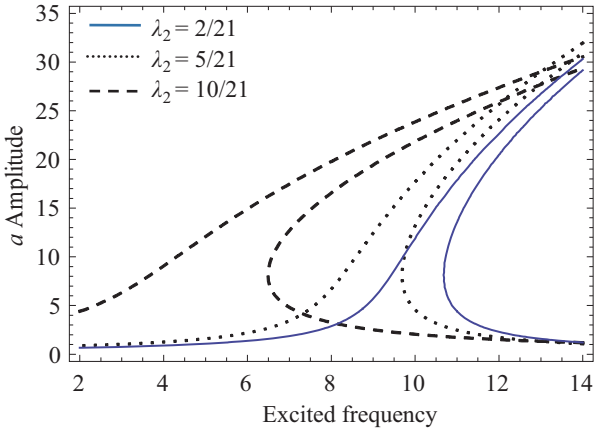


Fig. 6 Force-response curves of delaminated plate corresponding to different delamination depth.

From Figs. 5-6, it is observed that both the increases in delamination depth and delamination radius will decrease frequencies of the delaminated circular plate.

4. CONCLUSIONS

In the present work, with the semi-analytic method and multiple scales method, the effects of delamination radius and delamination depth on the natural frequency, mode shape and primary resonance behaviors of a delaminated circular plate are presented. The results show that delamination has considerable impact on the natural frequency and primary resonance behaviors of a delaminated circular plate. Based on the thorough study on the numerical results, the following main conclusions can be reached:

1. By introducing Bessel Function and Modified Bessel Function, semi-analytic method was applied in the analysis of the linear and nonlinear dynamic behaviors of a delaminated circular plate.
2. The natural frequencies of a delaminated circular plate decrease with the increase in delamination depth and delamination radius.
3. Both the delamination depth and radius affect the mode shape of a delaminated circular plate. In the case of small delamination radius, the global mode dominates the mode shape of a delaminated circular plate whatever the delamination depth is. Besides, the local mode will dominate the mode shape of a delaminated circular plate in the case of the large delamination radius and small delamination depth.
4. Both the delamination depth and radius affect the primary resonance behaviors of a delaminated circular plate. Both the increases in delamination radius and depth will increase the hardening type behaviors of the system of a circular delaminated plate.

https://doi.org/10.1017/jmech.2016.84 Published online by Cambridge University Press

ACKNOWLEDGEMENTS

The author gratefully acknowledges the support of the National Natural Science Foundation of China (NNSFC, No.11172051) and Hunan Provincial Natural Science Foundation of China (No. 2015JJ4006).

APPENDIX A

Substituting Eqs (15) and (16) into Eqs (12)-(14), we have

$$B_n^{II} = B_n^{III} = D_n^{II} = D_n^{III} = F_n^{II} = F_n^{III} = 0 \tag{A.1}$$

And

$$G_n^I(1) = 0 \tag{A.2}$$

$$F_n^I(1) = 0 \tag{A.3}$$

$$G_n^{I''}(1) + (\alpha_5^I - \bar{K})G_n^{I'}(1) = 0 \tag{A.4}$$

$$G_n^I(\rho_0) - G_n^{II}(\rho_0) = 0 \tag{A.5}$$

$$G_n^I(\rho_0) - G_n^{III}(\rho_0) = 0 \tag{A.6}$$

$$G_n^{I'}(\rho_0) - G_n^{II}{}'(\rho_0) = 0 \tag{A.7}$$

$$G_n^I{}'(\rho_0) - G_n^{III'}(\rho_0) = 0 \tag{A.8}$$

$$N_n(\tau)A - \Phi_n(\tau)B = 0 \tag{A.9}$$

$$N_n(\tau)C - \Phi_n(\tau)D = 0 \tag{A.10}$$

$$\Phi_n(\tau)E - N_n(\tau)F = 0 \tag{A.11}$$

$$F_n^I(\rho_0) = F_n^{II}(\rho_0) + F_n^{III}(\rho_0) \tag{A.12}$$

$$\beta_1^I G_n^I(\rho_0) = \beta_1^{II} G_n^{II}(\rho_0) + \beta_1^{III} G_n^{III}(\rho_0) \tag{A.13}$$

in which

$$\begin{aligned}
A &= (\alpha_3^{II} + \alpha_2^{II})F_n^{II}(\rho_0) + \alpha_2^{II}\rho_0 F_n^{II'}(\rho_0) - (\alpha_3^I + \alpha_2^I)F_n^I(\rho_0) + \alpha_2^I \rho_0 F_n^{I'}(\rho_0) \\
B &= \frac{1}{2}\beta_2^I \lambda_{III} F_n^{I'}(\rho_0) \\
C &= (\alpha_3^{III} + \alpha_2^{III})F_n^{III}(\rho_0) + \alpha_2^{III}\rho_0 F_n^{III'}(\rho_0) - (\alpha_3^I + \alpha_2^I)F_n^I(\rho_0) + \alpha_2^I \rho_0 F_n^{I'}(\rho_0) \\
D &= -\frac{1}{2}\beta_2^I \lambda_{II} F_n^{I'}(\rho_0) \\
E &= G_n^{I''}(\rho_0) + \frac{\alpha_{5,1}}{\rho_0}G_n^{I'}(\rho_0) - \left\{\alpha_{1,2}G_n^{II''}(\rho_0) + \frac{\alpha_{5,2}}{\rho_0}G_n^{II'}(\rho_0)\right\} - \left\{\alpha_{1,3}G_n^{III''}(\rho_0) + \frac{\alpha_{5,3}}{\rho_0}G_n^{III'}(\rho_0)\right\} \\
F &= \frac{1}{2}\left\{\frac{1}{\rho_0}\lambda_{III}F_n^{II}(\rho_0) - \frac{1}{\rho_0}\lambda_{II}F_n^{III}(\rho_0)\right\}
\end{aligned} \tag{A.14}$$

Due to the existence of time terms and 14 unknown variables, Eqs. (A.2-13) can't be solved directly. It is known that the axial force and shear force will be directly proportional to the height of *i*-region at the delamination front, and then α_n, A_n^I, B_n^I, C_n^I, D_n^I, A_n^{II}, C_n^{II}, and A_n^{III}, C_n^{III} can be obtained by using Eqs. (A.2,) (A.4), (A.5), (A.8), (A.13) and E in Eq. (A.14). As above, β_n and E_n^I, F_n^I, E_n^{II}, E_n^{III} can be derived by using Eqs. (A.3), (A.12) and A and D in Eq. (A.14).

APPENDIX B

$$a_{nk}^1 = -\left\{\int_{\rho_0}^1 \lambda_I G_n^I(\rho)G_k^I(\rho)d\rho + \int_0^{\rho_0}\lambda_{II}G_n^{II}(\rho)G_k^{II}(\rho)d\rho + \int_0^{\rho_0}\lambda_{III}G_n^{III}(\rho)G_k^{III}(\rho)d\rho\right\}$$

$$\begin{aligned}
a_{nk}^2 = -\Bigg\{&\int_{\rho_0}^1 \frac{1}{12\rho}\xi_I^2\lambda_I G_n^I{}'(\rho)G_k^I(\rho)d\rho + \int_{\rho_0}^1 \frac{1}{12}\xi_I^2\lambda_I G_n^I{}''(\rho)G_k^I(\rho)d\rho + \int_0^{\rho_0}\frac{1}{12\rho}\xi_{II}^2\lambda_{II}G_n^{II}{}'(\rho)G_k^{II}(\rho)d\rho \\
&+ \int_0^{\rho_0}\frac{1}{12}\xi_{II}^2\lambda_I G_n^{II}{}''(\rho)G_k^{II}(\rho)d\rho + \int_0^{\rho_0}\frac{1}{12\rho}\xi_{III}^2\lambda_{III}G_n^{III}{}'(\rho)G_k^{III}(\rho)d\rho + \int_0^{\rho_0}\frac{1}{12}\xi_{III}^2\lambda_I G_n^{III}{}''(\rho)G_k^{III}(\rho)d\rho\Bigg\}
\end{aligned}$$

$$a_{nk}^3 = -\left\{\int_{\rho_0}^1 c^I G_n^I(\rho)G_k^I(\rho)d\rho + \int_0^{\rho_0}c^{II}G_n^{II}(\rho)G_k^{II}(\rho)d\rho + \int_0^{\rho_0}c^{III}G_n^{III}(\rho)G_k^{III}(\rho)d\rho\right\}$$

https://doi.org/10.1017/jmech.2016.84 Published online by Cambridge University Press

$$a_{nmk}^{4} = \int_{\rho_0}^{1} \frac{1}{\rho} F_n^I{}'(\rho) G_m^I{}'(\rho) G_k^I(\rho) d\rho + \int_{\rho_0}^{1} \frac{1}{\rho} F_n^I(\rho) G_m^I{}''(\rho) G_k^I(\rho) d\rho + \int_{0}^{\rho_0} \frac{1}{\rho} F_n^{II}{}'(\rho) G_m^{II}{}'(\rho) G_k^{II}(\rho) d\rho$$
$$+ \int_{0}^{\rho_0} \frac{1}{\rho} F_n^{II}(\rho) G_m^{II}{}''(\rho) G_k^{II}(\rho) d\rho + \int_{0}^{\rho_0} \frac{1}{\rho} F_n^{III}{}'(\rho) G_m^{III}{}'(\rho) G_k^{III}(\rho) d\rho + \int_{0}^{\rho_0} \frac{1}{\rho} F_n^{III}(\rho) G_m^{III}{}''(\rho) G_k^{III}(\rho) d\rho$$

$$a_{nk}^{5} = \int_{\rho_0}^{1} \alpha_1^I G_n^I{}''''(\rho) G_k^I(\rho) d\rho + \int_{\rho_0}^{1} \frac{2\alpha_1^I}{\rho} G_n^I{}'''(\rho) G_k^I(\rho) d\rho - \int_{\rho_0}^{1} \frac{\alpha_6^I}{\rho^2} G_n^I{}''(\rho) G_k^I(\rho) d\rho + \int_{\rho_0}^{1} \frac{\alpha_6^I}{\rho^3} G_n^I{}'(\rho) G_k^I(\rho) d\rho$$
$$+ \int_{0}^{\rho_0} \alpha_1^{II} G_n^{II}{}''''(\rho) G_k^{II}(\rho) d\rho + \int_{0}^{\rho_0} \frac{2\alpha_1^{II}}{\rho} G_n^{II}{}'''(\rho) G_k^{II}(\rho) d\rho - \int_{0}^{\rho_0} \frac{\alpha_6^{II}}{\rho^2} G_n^{II}{}''(\rho) G_k^{II}(\rho) d\rho$$
$$+ \int_{0}^{\rho_0} \frac{\alpha_6^{II}}{\rho^3} G_n^{II}{}'(\rho) G_k^{II}(\rho) d\rho + \int_{0}^{\rho_0} \alpha_1^{III} G_n^{III}{}''''(\rho) G_k^{III}(\rho) d\rho + \int_{0}^{\rho_0} \frac{2\alpha_1^{III}}{\rho} G_n^{III}{}'''(\rho) G_k^{III}(\rho) d\rho$$
$$- \int_{0}^{\rho_0} \frac{\alpha_6^{III}}{\rho^2} G_n^{III}{}''(\rho) G_k^{III}(\rho) d\rho + \int_{0}^{\rho_0} \frac{\alpha_6^{III}}{\rho^3} G_n^{III}{}'(\rho) G_k^{III}(\rho) d\rho$$

$$a_{nk}^{6} = T_s \left\{ \int_{\rho_0}^{1} \frac{1}{12\rho} \xi_I^2 \lambda_I G_n^I{}'(\rho) G_k^I{}'(\rho) d\rho + \int_{0}^{\rho_0} \frac{1}{12\rho} \xi_{II}^2 \lambda_{II} G_n^{II}{}'(\rho) G_k^{II}{}'(\rho) d\rho + \int_{0}^{\rho_0} \frac{1}{12\rho} \xi_{III}^2 \lambda_{III} G_n^{III}{}'(\rho) G_k^{III}{}'(\rho) d\rho \right\}$$

$$a_{nk}^{7} = \int_{\rho_0}^{1} \beta_1^I G_n^I{}'(\rho) G_k^I{}'(\rho) d\rho - T_s \int_{\rho_0}^{1} \alpha_1^I G_n^I{}'''(\rho) G_k^I{}'(\rho) d\rho - -T_s \int_{\rho_0}^{1} \frac{\alpha_1^I}{\rho} G_n^I{}''(\rho) G_k^I{}'(\rho) d\rho$$
$$+ T_s \int_{\rho_0}^{1} \frac{\alpha_6^I}{\rho^2} G_n^I{}'(\rho) G_k^I{}'(\rho) d\rho + \int_{0}^{\rho_0} \beta_1^{II} G_n^{II}{}'(\rho) G_k^{II}{}'(\rho) d\rho - T_s \int_{0}^{\rho_0} \alpha_1^{II} G_n^{II}{}'''(\rho) G_k^{II}{}'(\rho) d\rho$$
$$- -T_s \int_{0}^{\rho_0} \frac{\alpha_1^{II}}{\rho} G_n^{II}{}''(\rho) G_k^{II}{}'(\rho) d\rho + T_s \int_{0}^{\rho_0} \frac{\alpha_6^{II}}{\rho^2} G_n^{II}{}'(\rho) G_k^{II}{}'(\rho) d\rho + \int_{0}^{\rho_0} \beta_1^{III} G_n^{III}{}'(\rho) G_k^{III}{}'(\rho) d\rho$$
$$- T_s \int_{0}^{\rho_0} \alpha_1^{III} G_n^{III}{}'''(\rho) G_k^{III}{}'(\rho) d\rho - T_s \int_{0}^{\rho_0} \frac{\alpha_1^{III}}{\rho} G_n^{III}{}''(\rho) G_k^{III}{}'(\rho) d\rho + T_s \int_{0}^{\rho_0} \frac{\alpha_6^{III}}{\rho^2} G_n^{III}{}'(\rho) G_k^{III}{}'(\rho) d\rho$$

$$a_{nk}^{8} = \int_{\rho_0}^{1} \beta_1^I G_n^I{}'(\rho) G_k^I{}'(\rho) d\rho + \int_{0}^{\rho_0} \beta_1^{II} G_n^{II}{}'(\rho) G_k^{II}{}'(\rho) d\rho + \int_{0}^{\rho_0} \beta_1^{II} G_n^{II}{}'(\rho) G_k^{II}{}'(\rho) d\rho$$

$$a_{nk}^{9} = \int_{\upsilon_0}^{1} \alpha_2^I \rho F_n^I{}''(\rho) F_k^I(\rho) d\rho + \int_{\rho_0}^{1} 3\alpha_2^I F_n^I{}'(\rho) F_k^I(\rho) d\rho + \int_{\rho_0}^{1} (\alpha_2^I - \alpha_4^I) \frac{1}{\rho} F_n^I(\rho) F_k^I(\rho) d\rho$$
$$+ \int_{0}^{\rho_0} \alpha_2^{II} \rho F_n^{II}{}''(\rho) F_k^{II}(\rho) d\rho + \int_{0}^{\rho_0} 3\alpha_2^{II} F_n^{II}{}'(\rho) F_k^{II}(\rho) d\rho + \int_{0}^{\rho_0} (\alpha_2^{II} - \alpha_4^{II}) \frac{1}{\rho} F_n^{II}(\rho) F_k^{II}(\rho) d\rho$$
$$+ \int_{0}^{\rho_0} \alpha_2^{III} \rho F_n^{III}{}''(\rho) F_k^{III}(\rho) d\rho + \int_{0}^{\rho_0} 3\alpha_2^{III} F_n^{III}{}'(\rho) F_k^{III}(\rho) d\rho + \int_{0}^{\rho_0} (\alpha_2^{III} - \alpha_4^{III}) \frac{1}{\rho} F_n^{III}(\rho) F_k^{III}(\rho) d\rho$$

$$a_{nmk}^{10} = \int_{\rho_0}^{1} \frac{1}{2} \beta_2^I G_n^I{}'(\rho) G_m^I{}'(\rho) F_k^I(\rho) d\rho + \int_{0}^{\rho_0} \frac{1}{2} \beta_2^{II} G_n^{II}{}'(\rho) G_m^{II}{}'(\rho) F_k^{II}(\rho) d\rho + \int_{0}^{\rho_0} \frac{1}{2} \beta_2^{III} G_n^{III}{}'(\rho) G_m^{III}{}'(\rho) F_k^{III}(\rho) d\rho$$

$$F_k(\tau) = \int_{\rho_0}^{1} \overline{q}(\rho, \tau) G_k^{II}(\rho) d\rho + \int_{0}^{\rho_0} \overline{q}(\rho, \tau) G_k^I(\rho) d\rho$$

REFERENCES

1. Saravanis, D. A. and Hopkins, D. A., "Effects of delaminations on the dynamic characteristics of composite laminates analysis and experiment," *Journal of Sound and Vibration*. **192**, pp. 977-993 (1996).
2. Ramkumar, R. L., Kulkarni, S. V. and Pipes, R. B., "Free Vibration Frequencies of a Delaminated Beam," *34th Annual Technical Conference Proceedings*, Society of Plastic Industry Inc., **Sec. 22-E**, pp. 1-5 (1979).
3. Wang, J. T. S., Liu, Y. Y. and Gibby, J. A., "Vibration of split beams," *Journal of Sound of Vibration*, **84**, pp. 491-502 (1982)
4. Luo, S. N., Fu, Y. M. and Cao, Z. Y., "Non-linear vibration of composite beams with an arbitrary delamination," *Journal of Sound of Vibration*, **271**, pp. 535-545 (2004)
5. Mujumdar, P. M. and Suryanarayan, S., "Flexural

https://doi.org/10.1017/jmech.2016.84 Published online by Cambridge University Press

vibrations of beams with delaminations," *Journal of Sound of Vibration*, **125**, pp. 441-461 (1988).

6. Shu, D. and Fan, H., "Free Vibration of a Bimaterial Split Beam," *Composites: Part B*, **27**, pp. 79-84 (1996).
7. Hu, J. S. and Hwu, C., "Free Vibration of Delaminated Composite Sandwich Beams," *AIAA Journal*, **33**, pp. 1911-1918 (1995).
8. Luo, H. and Hanagud, S. "Dynamics of delaminated beams," *International Journal of Solids and Structures*, **37**, pp. 1501-1519 (2000).
9. Qiao, P. H. and Chen, F. L., "On the improved dynamic analysis of delaminated beams," *Journal of Sound and Vibration*, **331**, pp. 1143-1163 (2013).
10. Chen, H. P., "Free vibration of prebucked and postbuckled plates with delamination," *Computer Science and Technology*, **51**, pp. 451-462 (1994).
11. Zak, A., Krawczuk, M. and Ostachowicz, W., "Vibration of a laminated composite plate with closing delamination," *Journal of intelligent Material System Structures*, **12**, pp. 545-551 (2001).
12. Shiau, L. C. and Zeng, J. Y., "Free vibration of rectangular plate with delamination," *Journal of Mechanics*, **26**, pp. 87-93 (2010).
13. Kumar, S. K., Cinefra, M., Carrera, E. and Ganguli R, Harursampath D. "Finite element analysis of free vibration of the delaminated composite plate with variable kinematic multilayered plate elements," *Composites: Part B*, **66**, pp. 453-465 (2014).
14. Hu, N., Fukunage, H., Kameyama, M., Aramaki, Y. and Chang, F. K., "Vibration analysis of delamination composite beams and plates using higher order finite element," *International Journal of Mechanical Science*, **44**, pp. 1479-1503 (2002).
15. Yam, L. H., Wei, Z., Cheng, L. and Wong, W. O., "Numerical analysis of multi-layer composite plates with internal delamination," *Computers and Structures*, **82**, pp. 627-637 (2004).
16. Chen, J., Wang, H. and Qing, G. H., "Modeling vibration behavior of delaminated composite laminates using meshfree method in Hamiltion system," *Applied Mathematics and Mechanics*, **36**, pp. 633-654 (2015).
17. Chen, D. L. and Fu Y. M., "Nonlinear dynamic response of an axisymmetrically -delaminated circular plate with considering contact effect," *Acta Mech Solida Sinica*, **28**, pp. 406-410 (2007).
18. Kim, C. S. and Dickinson, S. M., "On the free, transverse vibration of annuar and circular, thin, sectorial plates subject to certain complicating effects," *Journal of Sound and Vibration*, **134**, pp. 407-421 (1989).
19. Nayfeh, A. H. and Mook, D. T., *Nonlinear Oscillations*, John Wiley & Sons, New York (1979).

(Manuscript received September 22, 2015,
accepted for publication May 1, 2016.)

https://doi.org/10.1017/jmech.2016.84 Published online by Cambridge University Press